УДК 621.437.048.001.2+621.45.072.3.048.001.5

F. THOUVEREZ, E. SARROUY

Ecole Centrale de Lyon, Laboratory of Tribology and System Dynamics, France

PERIODIC SOLUTION ANALYSIS OF A ROTOR-STATOR CONTACT NONLINEAR PROBLEM

A typical problem encountered when studying turbo-machineries is studied: contact between a rotor and his stator. The contact is supposed to be permanent and frictionless. Nonlinear vibrations appear through the geometry of the problem when it is excited by an out-of-balance within the rotor. Equations are written in the rotating frame. The stability and bifurcation analysis of a particular equilibrium is carried on and exhibits two Hopf bifurcation points. The associated periodic solutions are constructed and followed, using a shooting method. A specific bifurcation diagram is then established.

bifurcation, stability, shooting method, continuation, nonlinear

1. Geometry, hypothesis and equations

The problem parameters are given on fig. 1.

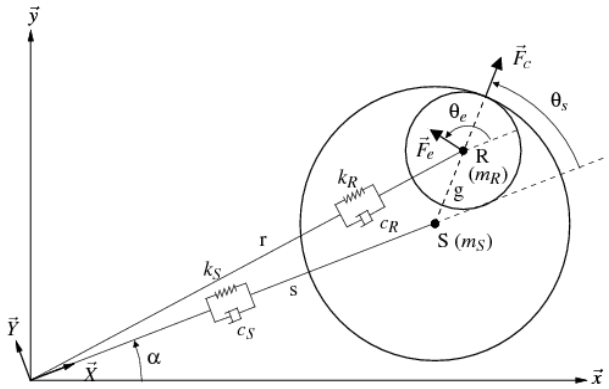

Fig. 1. Model and notations

Equations are written under the following assumptions:

1. Frictionless and permanent contact between rotor and stator, which implies that $\vec{F}_c$ and $\overrightarrow{SR}$ are aligned and the constrain $\vec{r} = \vec{s} + g(\cos\theta_s \vec{X} + \sin\theta_s \vec{Y})$.

2. Gyroscopic effects can be neglected.

Equations in the rotating frame $\vec{X}\vec{Y}$, assuming a viscous damping form, are:

$$m_R(\ddot{s} - g(\ddot{\theta}_s + \ddot{\alpha})\sin\theta_s - g(\dot{\theta}_s + \dot{\alpha})^2\cos\theta_s - s\dot{\alpha}^2) = \\ = -c_R(\dot{s} - g(\dot{\theta}_s + \dot{\alpha})\sin\theta_s - k_R(s + g\cos\theta_s) + \\ + F_e\cos\theta_e - F_c\cos\theta_c; \quad (1)$$

$$m_R(s\ddot{\alpha} - g(\ddot{\theta}_s + \ddot{\alpha})\cos\theta_s + 2\dot{s}\dot{\alpha} - g(\dot{\theta}_s + \dot{\alpha})^2\sin\theta_s) = \\ = -c_R(s\dot{\alpha} + g(\dot{\theta}_s + \dot{\alpha})\cos\theta_s) - k_R(g\sin\theta_s) + \\ + F_e\sin\theta_e - F_c\cos\theta_c; \quad (2)$$

$$m_s(\ddot{s} - s\dot{\alpha}^2) = -c_s\dot{s} - k_s s + F_c\cos\theta_s; \quad (3)$$

$$m_s(\ddot{\alpha} - 2s\dot{s}\dot{\alpha}) = -c_s s\dot{\alpha} + F_c\sin\theta_s. \quad (4)$$

The out-of-balance excitation is given by:

$$\vec{F}_e = F_e(\cos\theta_s\vec{X} + \sin\theta_s\vec{Y}), \quad (5)$$

where $\vartheta_e(t) = (2\pi f_e)t - \alpha(t)$.

By collecting equations (1) – (4), the following augmented and autonomous system is defined to describe the problem:

$$\dot{x} = F(x, f_e) = \left\{\dot{\hat{s}}, \dot{\hat{\theta}}_s, (2\pi f_e) - \dot{\hat{\alpha}}, G^t(x, f_e)\right\}^t; \\ x = \left\{s, \theta_s, \theta_e, \hat{s}, \hat{\theta}_s, \hat{\alpha}\right\}^t, \quad (6)$$

where $G(x, f_e) = B(x)^{-1}\tilde{F}(x, f_e)$.

$$B(x) = \begin{vmatrix} m_R + m_s & -m_R g\sin\theta_s & -m_R g\sin\theta_s \\ 0 & -m_R g\cos\theta_s & -m_R g\cos\theta_s + (m_R + m_s)s \\ m_s\tan\theta_s & 0 & -m_s s \end{vmatrix};$$

$$\tilde{F}(x, f_e) = \begin{vmatrix} (m_R + m_s)s\dot{\alpha}^2 + gm_R(\dot{\theta}_s + \dot{\alpha})^2\cos\theta_s - s\dot{\alpha}^2 - \ldots \\ \ldots(c_R + c_s)\dot{s} + c_R(\dot{\theta}_s + \dot{\alpha})^2 g\sin\theta_s - \ldots \\ \ldots(k_R + k_s)s - k_R\cos\theta_s + F_e\cos\theta_e \\ (-2m_R - 2m_s)\dot{s}\dot{\alpha}^2 + gm_R(\dot{\theta}_s + \dot{\alpha})^2\sin\theta_s - \ldots \\ \ldots(c_R + c_s)g\cos\theta_s + c_R(\dot{\theta}_s + \dot{\alpha})^2 g\sin\theta_s \ldots \\ -k_R g\sin\theta_s + F_e\sin\theta_e \\ 2m_s s\dot{\alpha}^2\tan\theta_s + 2m_s\dot{s}\dot{\alpha} - c_s(\dot{s}\tan\theta_s - s\dot{\alpha}) - k_s s\tan\theta_s \end{vmatrix}.$$

2. Classical bifurcation diagram

We first established a classical bifurcation diagram by sampling the system response with a frequency equal

to the excitation one. The time integration scheme is a Newmark one with constant acceleration approximation ($\gamma = 1/2, \beta = 1/4$). The algorithm can be found in [1]. The result is shown on fig. 2. This diagram exhibits a fixed point or a synchronous periodic solution and then shows a quasi-periodic or non-synchronous solution before coming back to an equilibrium or synchronous state. In order to describe the system behaviour in a more accurate way, we led a full analysis.

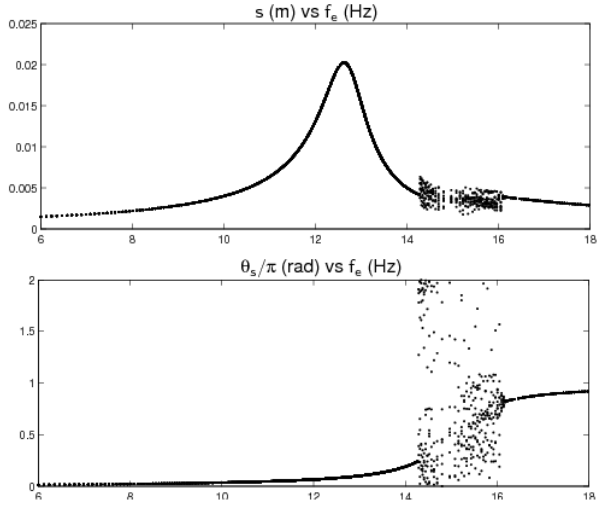

Fig. 2. Classical bifurcation diagram

3. Fixed point analysis

We look for x such that $F(x, f_e) = 0$: rotor and stator are fixed in the rotating frame.

Equations (1) – (4) become simpler:

$$m_R(2\pi f_e)^2 \cos\theta_s - k_R(s + g\cos\theta_s) - \\ - c_R(2\pi f_e) g \sin\theta_s - F_e \cos\theta_s - F_c \cos\theta_e = 0; \quad (7)$$

$$(m_R(2\pi f_e)^2 - k_R) g \cos\theta_s - \\ - c_R(2\pi f_e)(s + g\sin\theta_s) - F_c \sin\theta_s + F_e \sin\theta_e = 0; \quad (8)$$

$$(m_s(2\pi f_e)^2 - k_s) s + F_c \cos\theta_s = 0; \quad (9)$$

$$c_s(2\pi f_e) s + F_c \sin\theta_s = 0. \quad (10)$$

Putting the left-hand terms in a function, we can re-write Eqn. (7) – (10) in a condensed way:

$$H(y) = 0; \\ y = \{s, \theta_s, \theta_e, F_c, f_e\}^t = \{\tilde{x}^t, f_e\}^t \mapsto H(y). \quad (11)$$

3.1. Continuation. We used a tangent predictor scheme and a Moore-Penrose corrector. These methods are fully explained in [2, 3, 4] hence we only mention the main steps:

Step 1 - Prediction: Having $y_n = (x_n, f_{en})$, estimate of the next point $y_{n+1}^{(0)}$ along the tangent vector t_n:

$$y_{n+1}^{(0)} = y_n + h t_n \quad (12)$$

h is the steplength. We kept it constant and equal to 1.

Step 2 – Correction: The predicted point does not usually fulfil Eqn. (11) which is numerically checked through $\|H(y)\| < \varepsilon_{fp}$.

Assume that after k correction steps, $\|H(y)\| > \varepsilon_{fp}$.

Linearization of $H(y_{n+1}^{(k)} + \Delta_k) = 0$ gives:

$$D_y H(y_{n+1}^{(k)}) \Delta_k = -H(y_{n+1}^{(k)}).$$

$D_y H$ is not square so that we have either to add an equation to the system (pseudo-arclength method) or to use the Moore-Penrose pseudo inverse $D_y H(y_{n+1}^{(k)})^+$. The equation used for the correction step is:

$$y_{n+1}^{(k+1)} = y_{n+1}^{(k)} - D_y H(y_{n+1}^{(k)})^+ H(y_{n+1}^{(k)}). \quad (13)$$

This continuation scheme applied on the excitation range $f_e \in [6\ \ 19] Hz$ leads to fig. 3.

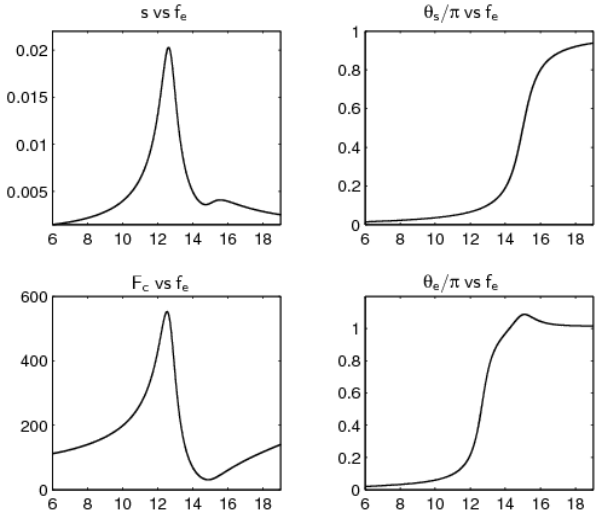

Fig. 3. Fixed point continuation

3.2. Stability. Equations to be considered are the non-simplified Eqn. (1) – (4). Stability study is achieved with the help of the eigenvalues λ_i of the Jacobian matrix $D_x F$. Stability criteria is all the real parts to be

negative. Figure 4 shows both real and imaginary parts of each six eigenvalues. This figure exhibit an unstable area [14.49 16.16] Hz that we will focus on.

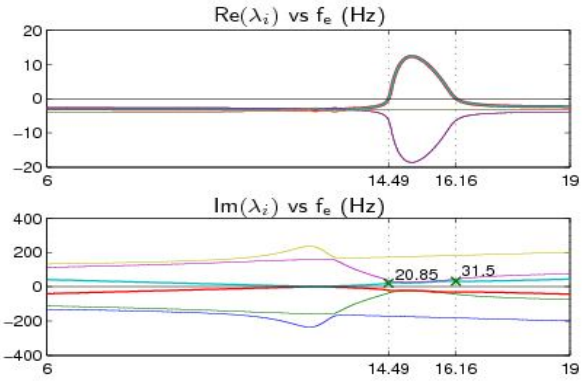

Fig. 4. Fixed point stability-Jacobian eigenvalues

3.3. Bifurcation analysis. This range provides two Hopf bifurcation points. In order to find out whether they are sub- or supercritical Hopf bifurcations, we compute the first Lyapunov number (see [3] for theory and computation steps).

In the first case ($f_e \approx 14{,}49\ Hz$), this number is positive. This means that the bifurcation is subcritical: it is a case of catastrophic bifurcation which requires a global analysis to be carried on. In the second case ($f_e \approx 16{,}69\ Hz$), the first Lyapunov number is negative: it is a supercritical Hopf bifurcation.

4. Hopf bifurcation branches study

4.1. Branching. We aim to find for each bifurcation point a branch of points lying on limit cycles. A first order analysis of the evolution of a "small" perturbation $y(t)$ to the fixed point x_0 at the critical parameter value f_{eb} (14,49 Hz or 16,16 Hz) leads to: $y(t) \approx y_1 V_1 e^{\omega_1 t} + y_2 \overline{V}_2 e^{\omega_1 t}$ for t large enough, with $V_1 = \overline{V}_2$, eigenvectors associated to the pair of non zero imaginary eigenvalues $\lambda_1 = \overline{\lambda}_2 = \omega_1$. It means that the predicted limit cycle for $f_e = f_{eb} \pm \Delta f_e$ should be found by using an algorithm for periodic solution construction initialized with $T_s = 2\pi/\omega_1$ as the period guess and $x_{ini}(0) = x_0 + \varepsilon V_1, \varepsilon << 1$ as a point on limit cycle.

4.2. Periodic continuation scheme. Once a point is caught, a continuation method can be used. First we build a continuous periodicity test function in order to solve the angular periodicity problem. Then, we present the general algorithm.

4.2.1. Angular periodicity test. We have to check the signal periodicity. A problem comes from the use of angles: physically $\vartheta_s = 0$ and $\vartheta_s = 2\pi$ denote the same position whereas they are numerically different. The modulo function not being continuous enough, we decided to use the test function:

$$\left\{s, \theta_s, \theta_e, \hat{s}, \hat{\theta}_s, \hat{\alpha}\right\}^t \mapsto \left\{s, \cos(\theta_s) - 1, \cos(\theta_e) - 1, \hat{s}, \hat{\theta}_s, \hat{\alpha}\right\}^t .$$

Denoting $x_f = x(t = T_s)$ the solution of Eqn. (6) with the initial condition $x(0) = x_i$, the periodicity test that ensures $\mathrm{x_i}$ to be on a limit cycle with period T_s is:

$$\varphi(x_f - x_i) = 0 . \qquad (14)$$

4.2.2. General periodic continuation algorithm. There are two main points: the prediction/correction scheme used to find periodic solutions and the step-length adaptation scheme that saves computation time.

Predictor/Corrector scheme: $x_f = x(T_s, x_0, f_e)$ implies that with a small perturbation of the initial guess, the periodicity condition (14) becomes:

$$\varphi(x_f(T_s + \Delta T_s, x_0 + \Delta x_0, f_e + \Delta f_e) - (x_0 + \Delta x_0)) = 0 . \qquad (15)$$

The first order development of Eqn. (15) gives:

$$\begin{aligned} &\varphi(x_f(T_s, x_0, f_e) - (x_0)) + \\ &+ D_x \varphi(x_f(T_{ss}, x_0, f_e) - (x_0)) \times \\ &\times \left[\frac{\partial x_f}{\partial T_s} \Delta T_s + (\frac{\partial x_f}{\partial x_0} - 1) \Delta x_0 + \frac{\partial x_f}{\partial f_e} \Delta f_e \right] = 0. \end{aligned} \qquad (16)$$

We can use Eqn. (16) either for prediction or correction:

– *Prediction case:* Assume that we possess $z_n = \{T_{sn}, x_{0n}^t, f_{en}\}^t$ satisfying Eqn. (6) and the periodicity condition (14), and that we want to predict $z_{n+1}^{(0)} = z_n + \{\Delta T_s, x_0^t, f_e\}^t = z_n + \Delta z$. Eqn. (16) provides:

$$\begin{aligned} &D_x \varphi(x_{fn} - x_{0n}) \times \\ &\times \left[\frac{\partial x_f}{\partial T_s} \Delta T_s + (\frac{\partial x_f}{\partial x_0} - 1) \Delta x_0 + \frac{\partial x_f}{\partial f_e} \Delta f_e \right] = 0. \end{aligned}$$

We need to add an equation or to delete an unknown component. We choose to force Δx_0 to be orthogonal to $F(x_{fn}, f_{en})$. Equations to be solved are then:

$$\begin{cases} \begin{bmatrix} D_x\varphi \dfrac{\partial x_f}{\partial T_s} & D_x\varphi \dfrac{\partial x_f}{\partial x_0} \\ 0 & F(x_{fn}, f_{en}) \end{bmatrix} \begin{Bmatrix} \Delta T_s \\ \Delta x_0 \end{Bmatrix} + \begin{Bmatrix} D_x\varphi \dfrac{\partial x_f}{\partial f_e} \\ 0 \end{Bmatrix} = 0; \\ \left\| \Delta z \right\| = h, \det\left(\begin{bmatrix} Ab \\ \Delta z^t \end{bmatrix} \right) > 0. \end{cases} \quad (18)$$

Values of partial derivatives $\dfrac{\partial x_f}{\partial T_s}, \dfrac{\partial x_f}{\partial x_0}, \dfrac{\partial x_f}{\partial f_e}$ at the point z_n can be obtained by time integration of partial differential equations [2].

– *Correction case (shooting method):* $z_n^{(i)}$ was evaluated and has to be corrected because $\varphi(x_{fn+1}^{(i)} - x_{0n+1}^{(i)}) = \delta^{(i)}, \delta^{(i)} \neq 0$ (numerically $\left\| \delta^{(i)} \right\| > \varepsilon_{test}$). f_{en+1} is kept constant and equal to the predicted value:

$$f_{en+1} = f_{en+1}^{(0)}. \quad (19)$$

Equation (16) then provides:

$$D_x\varphi(x_{fn+1}^{(i)} - x_{0n+1}^{(i)}) \times \times \left[\frac{\partial x_f}{\partial T_s} \Delta T_s + (\frac{\partial x_f}{\partial x_0} - 1)\Delta x_0 + \frac{\partial x_f}{\partial f_e} \Delta f_e \right] = -\delta^{(i)}. \quad (20)$$

The same missing equation than for the prediction step was chosen :

$$z_n = \{\Delta T_s, \Delta x_0^t\} F(x_{fn+1}^{(i)}, f_{en+1}). \quad (21)$$

Steplength adaptation: Such a control scheme permits to save computation time by optimizing the parameter h mentionned in Eqn. (18). h value is adapted depending on the number of correction iterations. If $i > i_{\max}$ the prediction was not accurate enough. Correction step is interrupted and a new prediction is made, using h/2. If correction test is achieved in a few iterations only, $i < i_{\min}$, the predicted point could have been farer from the previous one. The next prediction will use a larger value for h, for example 2h.

4.3. Floquet multipliers analysis. Using the method exposed previously we caught both periodic solutions predicted by both Hopf bifurcations. Then we used the continuation scheme which we described and we obtained the results showed in fig. 5 and fig. 6. The circle denotes the bifurcation point. The upper curve (a) is related to the periodic solution frequency $f_s = 1/T_s$. As can be observed they are non-synchronous solutions and moreover the frequency evolves without following any simple rule. The lower curve (b) represents the leading Floquet multiplier modulus. Floquet multipliers are eigenvalues of the monodromy matrix obtained as computational by-product of the shooting method. To make the figures more comprehensible we only drew the Floquet multiplier responsible for the unstability, which is the one whose modulus crosses the line $y = 1$.

Fig. 5 shows that the periodic solution near the bifurcation point is unstable. Then we observe a turning point and stability is gained.

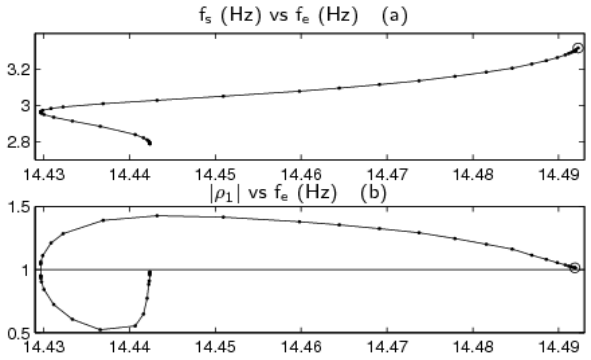

Fig. 5. Subcritical Hopf bifurcation
Continuation of the unstable periodic solution

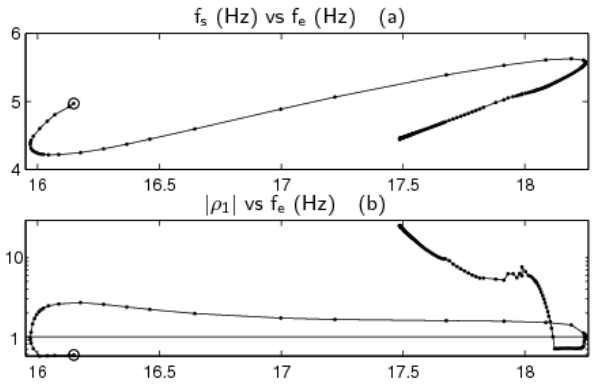

Fig. 6. Supercritical Hopf bifurcation – Continuation of the stable periodic solution

Fig. 6 shows a more complex behaviour: as predicted by the supercritical aspect of the second Hopf

bifurcation, the solution is stable near the bifurcation point. Then a turning point is reached and stability is lost ($f_e \approx 15{,}97\ Hz$) and vice-versa for $f_e \approx 18{,}25\ Hz$. Finally, a period doubling bifurcation occurs for $f_e \approx 18{,}11\ Hz$. We built this solution but chose not to show it because it quickly undergoes Hopf bifurcation that would lead to a quasi-periodic solution.

Subcritical Hopf bifurcation being a catastrophic one, we seek a stable solution above the critical excitation value $f_e \approx 14{,}49\ Hz$.

5. Search for a disconnected solution

In order to find a stable solution disconnected from the unstable fixed point, we increased f_e from a small amount and led a time integration. The solution to which the system hung was a periodic non-synchronous one. Fig. 7 shows the response frequency versus the excitation one. Amplitudes are of the same order than previously but this family of periodic solutions has a contact force doing some incursions into the negative values. Besides, this branch of periodic solutions has many bifurcations. We did not represent the Floquet multipliers because the curves were hardly legible.

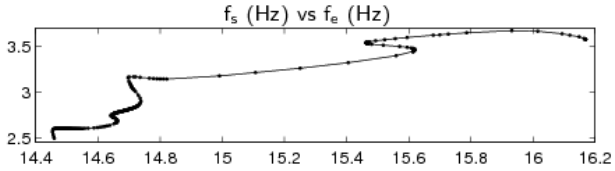

Fig. 7. Global analysis – Continuation of a disconnected solution

6. New bifurcation diagram

In view of the complexity and high amount of information that need to be taken into account to fully understand and predict the system behaviour, it seemed that a new bifurcation diagram should be used. We propose one on fig. 8. It focus on the "bifurcation area". It portrays the response frequency in case of periodic solution (fig. 8, a) and the amplitudes of the solution (fig. 8, b). We chose the minimum and maximum values reached during a period as amplitudes representation for periodic solutions. Symbols are used to link curves from both graphs and continuous and discontinuous lines are used to distinguish stable from unstable states respectively.

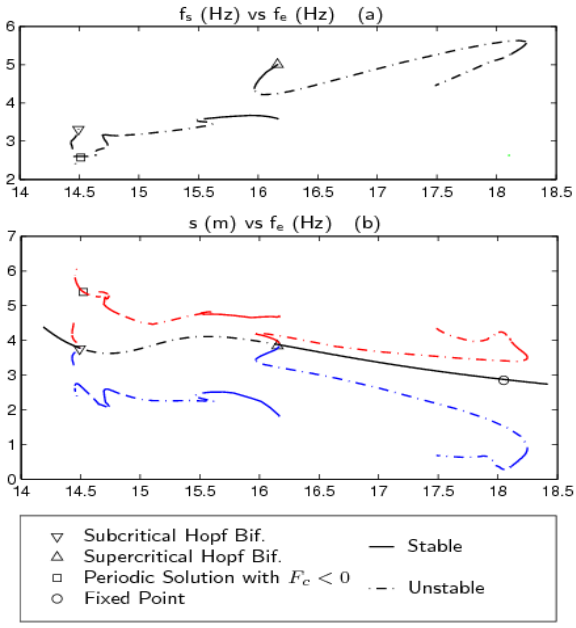

Fig. 8. New bifurcation diagram

Conclusion

This simple system proved to have a complex behaviour with many bifurcations. Our initial choice to write equations in the rotating frame simplifies the results and their analysis. Moreover, this work emphasizes that a simple (classical) bifurcation diagram is not efficient at describing complex behaviour. We proposed a new way of representing information.

References

1. Géradin M., Rixen D. Théorie des Vibrations // Masson. – 1993.

2. Nayfeh A.H., Balachandran B. Applied Nonlinear Dynamics // Wiley. – 1995.

3. Kuznetsov Yuri A. Elements of Applied Bifurcation Theory, 3rd ed. // Springer. – 2004.

4. Allgower E.L., Georg K. Introduction to Numerical Continuation Methods // Springer. – 2003.

Поступила в редакцию 13.06.2006

Рецензент: д-р техн. наук, проф. В.В. Панин, Национальный авиационный университет, Киев.